Transition to Detonation in Non-Uniform H_2–Air: Chemical Kinetics of Shock-Induced Strong Ignition

L. R. Boeck, J. Hasslberger and T. Sattelmayer
Lehrstuhl für Thermodynamik, Technische Universität München
Garching, Germany

1 Introduction

Extensive knowledge is available on explosions in homogeneous gas mixtures. Mixtures of H_2 and air have been investigated particularly in the context of nuclear reactor safety. However, a major current knowledge gap concerns the influence of mixture inhomogeneity. Spatial concentration gradients are omnipresent in real-world accident scenarios. We address this knowledge gap experimentally, reducing complexity by investigating one-dimensional concentration gradients. Gradients are oriented perpendicular to the main direction of explosion front propagation, thus termed "transverse concentration gradients".

DDT can be split up into flame acceleration (FA) and the actual transition to detonation, often called "onset of detonation". This distinction is of great help for understanding the physics of the specific processes. We studied the influence of gradients on FA separately [3], concluding that gradients can enforce FA significantly. This work however did not investigate transition to detonation. This sudden process, often described as an "explosion in the explosion", typically involves the formation of a blast wave from a violent local explosion that transforms into a detonation. Transition can be interpreted as a sequence of events, so that a chain of criteria needs to be satisfied for successful transition:

1. Formation of a hot spot and a local explosion event.
2. Formation of a detonation originating from the local explosion.
3. Propagation of the detonation front into the macroscopic confining geometry.

Interestingly, studies aiming at defining critical conditions for transition to detonation mostly do not address the physics and chemistry of step 1, but focus on secondary steps 2 and 3. Examples are a criterion by Thomas et al. [10], which describes the survival of a detonation formed at an obstacle surface (step 2), mitigated by the expansion fan originating at the obstacle edge, or the well-known empirical 7λ criterion by Dorofeev et al. [5], which defines a critical geometrical length scale for transition to detonation, thus mainly referring to step 3.

The present work suggests a different perspective, addressing the first and thus crucial step of transition to detonation, namely the formation of a local explosion generating a blast wave that subsequently may

Correspondence to: boeck@td.mw.tum.de

transform into a detonation. From a safety perspective, this is particularly relevant since local explosions cause the highest local overpressures observable in all explosion regimes (clearly beyond Chapman-Jouguet detonation overpressure), e.g. beyond 100 bar [4]. Obstructed channel configurations were investigated by means of highly time-resolved shadowgraphy, photodiode and pressure measurements. Computation of detailed chemical kinetics allows for defining critical conditions for local explosion occurence. The deduced criterion proves universal both for homogeneous and non-uniform H_2–air mixtures.

2 Experimental Setup

Experiments are conducted in an entirely closed rectangular explosion channel (length: 5.1 m; height: 0.06 m; width: 0.3 m), Fig. 1. The channel can be equipped with periodic flat plate obstacles with a blockage ratio BR = 2h/H at a spacing S.

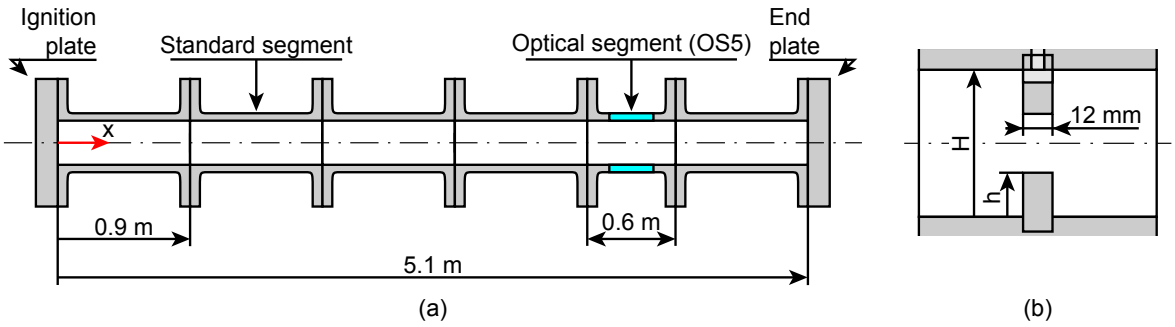

Figure 1: Schematic of experimental setup, top view (a). Obstacle geometry, side view (b).

Figure 2 illustrates the generation of transverse (vertical) concentration gradients. First, the channel is filled with ambient air. Then, the volume is partially evacuated. H_2 is injected through a regular pattern of 153 injection ports in the facility top plate (1).

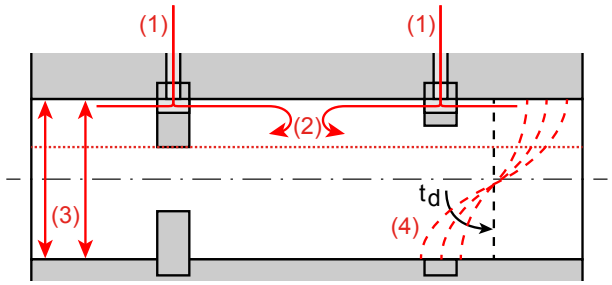

Figure 2: Generation of vertical H_2 concentration gradients.

The H_2 flow is deflected inside the channel, forming a compact horizontal H_2 layer along the channel top (2). At obstacle positions in the obstructed channel section, H_2 deflection is achieved by slots in the upper obstacles. Positions between obstacles are equipped with manifolds protruding into the channel at the upper wall. These manifolds do not significantly influence the DDT process [2]. Vertical concentration gradients form by diffusion (3). The resulting gradients (4) are oriented vertically. Gradients of defined slope can be generated by controlling the diffusion time t_d between H_2 injection and ignition. A diffusion time of 60 s yields homogeneous mixtures, whereas a diffusion time of 3 s results in steep concentration gradients. Pressure prior to ignition is atmospheric, temperature equals the laboratory temperature. For further details on the experiment please refer to [2].

3 Mechanism of Transition to Detonation

The general transition mechanism in obstructed channel configurations is depicted in Fig.3 for a homogeneous mixture. A shock at a velocity of 1000 m/s propagates towards a BR30 obstacle. The shock is reflected off the obstacle between t = 12.5 and 25 μs. Primary local explosions can be observed both at the upper and lower obstacle. The image at t = 50 μs shows collision of the explosion fronts at the channel center line. Subsequent images do not allow for clear tracking of the fronts during diffraction around the obstacle. Eventually, the detonation front emerges clearly at t = 112.5 μs at the channel bottom. Detonation is initiated by the formation of a secondary hot spot at the lower channel wall. In mixtures with concentration gradients, the general mechanism of transition to detonation is similar. Primary local explosions are mostly observed at the channel top, thus in the most fuel-rich region. Figure 4 gives an example out of more than 200 similar optical measurements conducted. Also at higher average H_2 concentrations, the local explosions at the channel top are responsible for transition to detonation [2].

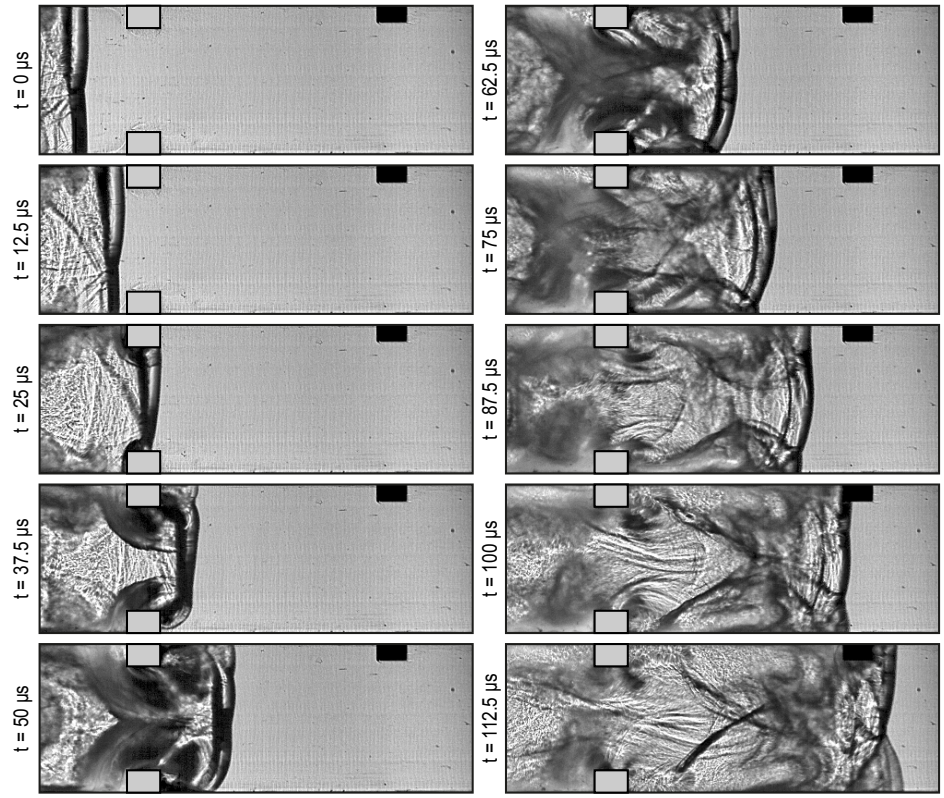

Figure 3: Transition to detonation in 16.5 vol. % H_2, homogeneous, BR30S300.

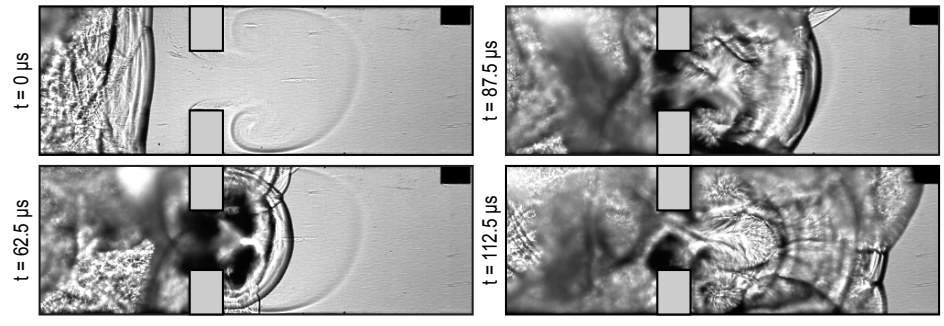

Figure 4: Transition to detonation in 22.5 vol. % H_2, gradient t_d = 3 s, BR60S300.

4 Strong Post-Reflected Shock Ignition

We analyze transition to detonation by means of post-reflected-shock detailed chemical kinetics simulations. Depending on blockage ratio and spacing, shock focusing and reflection of Mach stems may occur in obstructed channels. Due to the large spacing of 0.3 m in configurations discussed in the present work, these effects are not pronounced so that nearly normal shocks interact with obstacles here. Thus, reflection of a normal shock off a solid wall is considered in one dimension. The extended second explosion limit is taken as a boundary between mild and strong ignition as proposed by Belles [1]. Strong ignition leads to local explosion. In contrast to Belles, we use detailed chemical kinetics simulations (Cantera [6], reaction mechanism by Ó Conaire et al. [8]) to determine the limit following an approach suggested by Shepherd [9]: The location of the extended second explosion limit in terms of temperature and pressure is determined by computing the reduced effective activation energy θ by numerical differentiation:

$$\theta = \frac{E_a}{RT} \approx \frac{1}{T} \frac{ln(\tau_{ind,+}) - ln(\tau_{ind,-})}{(1/T_+) - (1/T_-)}. \quad (1)$$

T is the initial mixture temperature, $\tau_{ind,+}$ and $\tau_{ind,-}$ are induction times computed for temperatures T_+ and T_-, respectively. Temperatures T_+ and T_- are gained by varying T by a factor of 1 ± 0.01.

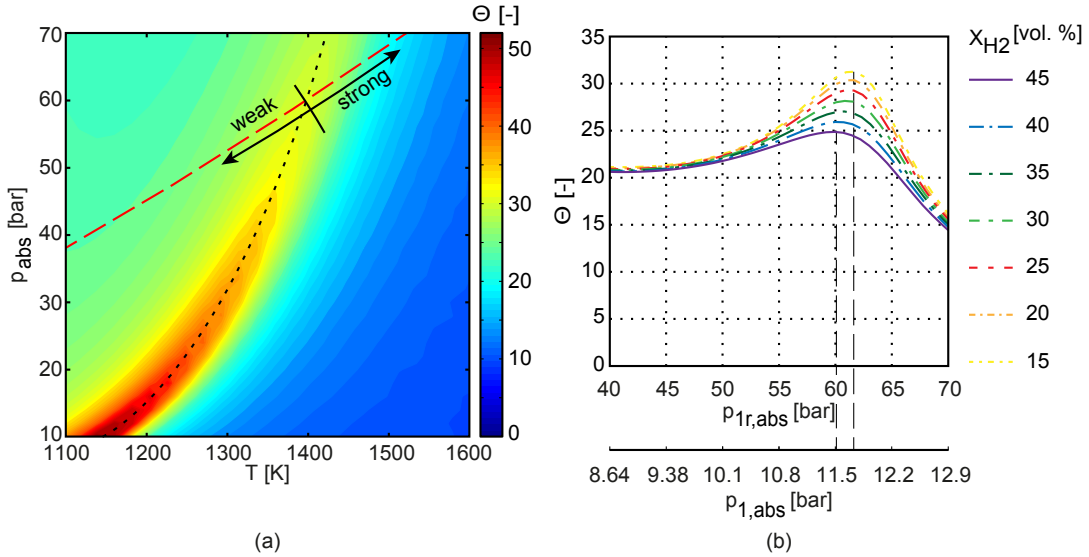

Figure 5: T-p plane of effective reduced activation energy θ (a); θ along post-reflected-shock states as a function of post-reflected (1r) and post-incident-shock (1) pressure (b).

The T–p plane for θ is depicted in color in Fig. 5 (a) for a 30 vol. % mixture. The region of maximum θ corresponds to the extended second explosion limit region (dotted black line marks line of maximum θ). Only specific T and p can occur behind a reflected shock. Valid post-reflected-shock states are described by reflected shock equations, dashed red line. This line is almost independent of H_2 concentration since $\gamma_{H_2} \approx \gamma_{air}$. The post-reflected-shock state needs to exceed the second extended explosion limit in order to cause strong ignition. Curves for θ as a function of post-reflected-shock pressure $p_{1r,abs}$ are shown in Fig. 5 (b). Absolute pressure is used here to be consistent with literature on explosion limits. The secondary axis of abscissas provides pressures behind incident shocks $p_{1,abs}$ that lead to corresponding post-reflected-shock pressures $p_{1r,abs}$. Between H_2 concentrations of 15 to 45 vol. %, the post-incident-shock pressure, which yields maximum θ after reflection, only varies between 11.5 and 11.8 bar (10.5–10.8 bar overpressure). Even if the extended second explosion limit is interpreted as a band rather than a sharp boundary, critical post-incident-shock overpressure lies in a narrow range of 10–11 bar.

The presented analysis of strong post-reflected-shock ignition so far suggests that:

- The pressure ratio of a fast deflagration precursor shock needs to exceed a critical value to allow for strong ignition after shock reflection.
- Critical post-incident-shock overpressure to cause strong ignition after shock reflection lies in a narrow range of 10–11 bar, which is almost independent of H_2 concentration.

Due to the minor influence of H_2 concentration on gasdynamic relations and chemical kinetics of strong ignition, conclusions can be directly transferred to mixtures with concentration gradients. Also here, post-reflected-shock overpressure and temperature need to exceed the extended second explosion limit locally to cause strong ignition.

Post-precursor-shock pressure of a fast deflagration can be related to flame Mach number, which is well measurable in experiments. Figure 6 shows results from an unobstructed channel configuration. If peak overpressure is depicted as a function of global flame Mach number Ma_F (sound speed calculated for reactants at average H_2 concentration), Fig. 6 (a), flames in gradient mixtures cause lower overpressure at given M_F than flames in homogeneous mixtures. Correlating both mixture types with local flame Mach number $\mathrm{M}_{F,y=0.06m}$ at the pressure measurement position (channel top), Fig. 6 (b), results coincide.

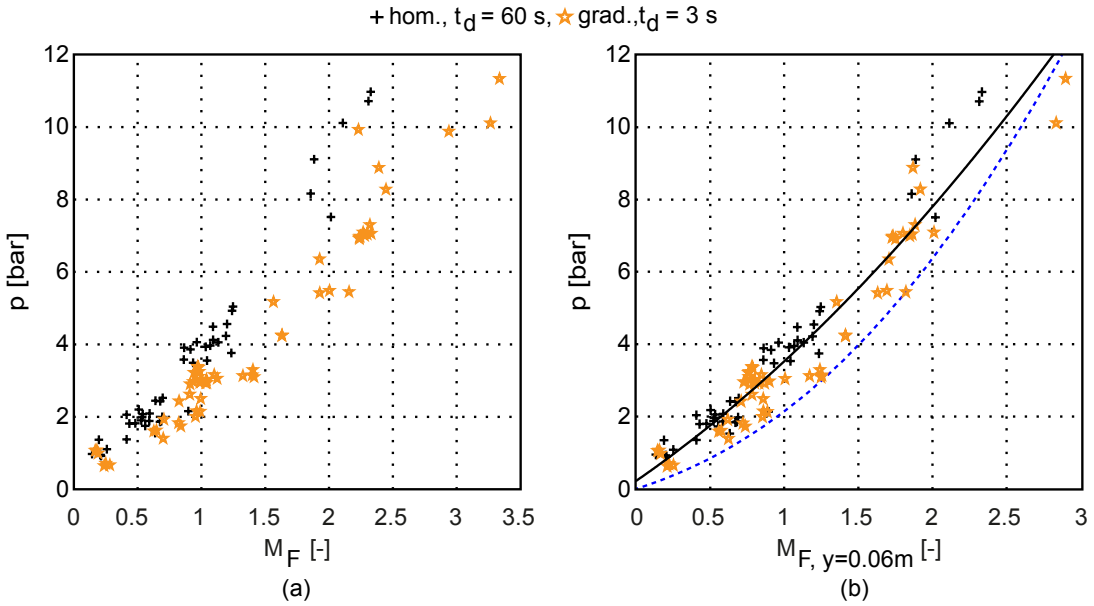

Figure 6: Relation of peak overpressure and global (a) / local (b) flame Mach number. Black line: experimental fit. Dashed blue line: 1D-model by Krok [7].

The relation between local flame Mach number and overpressure can be linked to the model for strong ignition behind a reflected shock. Since critical conditions for strong ignition can be expressed in terms of post-incident-shock overpressure, a critical local flame Mach number must be reached to achieve strong ignition and thus potentially transition to detonation. This proves true in both homogeneous and gradient mixtures. A 1D model of a shock-flame complex by Krok [7], dashed blue line in Fig. 6 (b), predicts a critical flame Mach number of 2.6–2.7 to reach post-incident-shock overpressure of 10–11 bar. Since this 1D model yields only a lower bound for realistic local overpressure due to its 1D character, these Mach numbers cannot portray a conservative boundary. Real local peak pressures tend to be higher. Critical local flame Mach number in experiments can therefore be estimated slightly lower at 2.4–2.6. Corresponding overpressure in the range of 10–11 bar is often observed shortly before transition to detonation in our experiments. This also implies that flames in mixtures with concentration gradiens need to accelerate to higher visible flame speeds (equal local flame Mach number) than flames in homogeneous mixtures to achieve transition to detonation.

5 Concluding Remarks

Transition to detonation in H_2–air mixtures was studied experimentally and by means of detailed chemical kinetics computations. We found that flames in both homogeneous mixtures and such with transverse concentration gradients need to accelerate to a critical local flame Mach number of the order of 2.4–2.6 to generate critical conditions for transition. Critical conditions were expressed in terms of critical overpressure behind the fast deflagration precursor shock. Employing the second extended explosion limit as a threshold between mild and strong ignition after shock reflection delivered critical overpressure values in the range of 10–11 bar, which is in very good agreement with our measurements.

Pronounced scatter in experimental data as visible in Fig. 6 clearly shows the stochastic nature of DDT: In single experiments—and of course in real-world explosions—local pressure can exceed values predicted by theoretical or experimental correlations. Critical flame Mach numbers determined here thus need to be understood as statistic mean values and be used only with an appropriate safety margin. Note that the approach using the extended second explosion limit could be extended towards more complex scenarios of shock-induced strong ignition, for example involving shock focusing.

The presented work is funded by the German Federal Ministry of Economic Affairs and Energy (BMWi) on the basis of a decision by the German Bundestag (project no. 1501338 and 1501425) which is gratefully acknowledged.

References

[1] Belles, F.E. (1958) Detonability and chemical kinetics: Prediction of limits of detonability of hydrogen. Symposium (International) on Combustion, vol. 7, pp. 745–751.

[2] Boeck, L.R. (2015) Deflagration-to-detonation transition and detonation propagation in H_2-air mixtures with transverse concentration gradients. Ph.D. Thesis, Technische Universität München.

[3] Boeck, L.R., Hasslberger, J., and Sattelmayer, T. (2014) Flame acceleration in hydrogen/air mixtures with concentration gradients. Combustion Science and Technology, vol. 186, pp. 1650–1661.

[4] Boeck, L.R., Hasslberger, J., Ettner, F. and Sattelmayer, T. (2013) Investigation of peak pressures during explosive combustion of inhomogeneous hydrogen–air mixtures. Proc of the 7^{th} International Seminar on Fire and Explosion Hazards. Providence, RI, USA.

[5] Dorofeev, S.B., Sidorov, V.P., Kuznetsov, M.S., Matsukov, I.D., and Alekseev, V.I. (2000) Effect of scale on the onset of detonations. Shock Waves, vol. 10, pp. 137–149.

[6] Goodwin, D.G., Moffat, H.K. and Speth, R.L. (2014) Cantera: An objectoriented software toolkit for chemical kinetics, thermodynamics, and transport processes. http://www.cantera.org, Version 2.1.2.

[7] Krok, J.C. (1991) One-dimensional flame propagation mechanisms.. Unpublished notes on the solution of ideal steady high-speed flames. RPI, Troy, NY.

[8] Ó Conaire, M., Curran, H. J., Simmie, J.M., Pitz, W. J., and Westbrook, C. K. (2004) A comprehensive modeling study of hydrogen oxidation. International Journal of Chemical Kinetics, vol. 36, pp. 603–622.

[9] Shepherd, J.E. (2009) Detonation in gases. Proceedings of the Combustion Institute, vol. 32, pp. 83–98.

[10] Thomas, G.O., Ward, S.M., Williams, R.L. and Bambrey, R.J. (2002) On critical conditions for detonation initiation by shock reflection from obstacles. Shock Waves, vol. 12, pp. 111–119.